Available online at www.sciencedirect.com
SCIENCE DIRECT
Biochimica et Biophysica Acta 1758 (2006) 181 – 189
BIOCHIMICA ET BIOPHYSICA ACTA
BBA
http://www.elsevier.com/locate/bba

Conformation and dynamics changes of bacteriorhodopsin and its D85N mutant in the absence of 2D crystalline lattice as revealed by site-directed ^{13}C NMR

Kazutoshi Yamamoto [a], Satoru Tuzi [a], Hazime Saitô [a,b,*], Izuru Kawamura [c], Akira Naito [c]

[a] Department of Life Science, Himeji Institute of Technology, University of Hyogo, Harima Science Garden City 678-1297, Japan
[b] Center for Quantum Life Sciences, Hiroshima University, Kagamiyama 1-chome, Higashi-Hiroshima, Japan
[c] Graduate School of Engineering, Yokohama National University, Tokiwadai, Hodogaya-ku, Yokohama, Japan

Received 2 November 2005; received in revised form 5 January 2006; accepted 31 January 2006
Available online 24 February 2006

Abstract

^{13}C NMR spectra of [3-^{13}C]Ala- and [1-^{13}C]Val-labeled D85N mutant of bacteriorhodopsin (bR) reconstituted in egg PC or DMPC bilayers were recorded to gain insight into their secondary structures and dynamics. They were substantially suppressed as compared with those of 2D crystals, especially at the loops and several transmembrane α_{II}-helices. Surprisingly, the ^{13}C NMR spectra of [3-^{13}C]Ala-D85N turned out to be very similar to those of [3-^{13}C]Ala-bR in lipid bilayers, in spite of the presence of globular conformational and dynamics changes in the former as found from 2D crystalline preparations. No further spectral change was also noted between the ground (pH 7) and M-like state (pH 10) as far as D85N in lipid bilayers was examined, in spite of their distinct changes in the 2D crystalline state. This is mainly caused by that the resulting ^{13}C NMR peaks which are sensitive to conformation and dynamics changes in the loops and several transmembrane α_{II}-helices of the M-like state are suppressed already by fluctuation motions in the order of 10^4–10^5 Hz interfered with frequencies of magic angle spinning or proton decoupling. However, ^{13}C NMR signal from the cytoplasmic α-helix protruding from the membrane surface is not strongly influenced by 2D crystal or monomer. Deceptively simplified carbonyl ^{13}C NMR signals of the loop and transmembrane α-helices followed by Pro residues in [1-^{13}C]Val-labeled bR and D85N in 2D crystal are split into two peaks for reconstituted preparations in the absence of 2D crystalline lattice. Fortunately, ^{13}C NMR spectral feature of reconstituted [1-^{13}C]Val and [3-^{13}C]Ala-labeled bR and D85N was recovered to yield characteristic feature of 2D crystalline form in gel-forming lipids achieved at lowered temperatures.

Keywords: Site-directed ^{13}C NMR; Conformation and dynamics change; 2D crystalline lattice; Bacteriorhodopsin; D85N

1. Introduction

Many integral membrane proteins are known to assemble into oligomeric complexes rather than monomers to form tertiary and quaternary structures necessary for biological signaling [1,2]. Such oligomeric complexes have been confirmed in view of the three-dimensional (3D) pictures of membrane proteins revealed by cryo-electron microscope or X-ray diffraction studies on two-dimensional (2D) or 3D crystals, including light-driven proton pump bacteriorhodopsin (bR) from purple membrane (PM) [3–5], phototaxis receptor sensory rhodopsin [6–8], photosynthetic reaction center [9], etc. In particular, bR from PM is know to present as a naturally occurring 2D crystal, in which stabilization energy is gained by specific lipid–protein interaction and protein–protein interactions among the transmembrane α-helices of neighboring molecules and endogenous lipid(s) as structural determinants [10]. Well-resolved high-resolution solid-state ^{13}C NMR signals were almost fully visible for bR labeled with [3-^{13}C]Ala- or [1-^{13}C]Val from fully hydrated PM: in fact, twelve ^{13}C Ala C_β, including the signals of five single carbons, and 9 Val C═O signals are well resolved among 29 Ala and 21 Val residues in the former and latter, respectively [11,12] by cross

* Corresponding author. Center for Quantum Life Sciences, Hiroshima University, Kagamiyama 1-chome, Higashi-Hiroshima, Japan. Fax: +81 78 856 2876.
E-mail address: hsaito@siren.ocn.ne.jp (H. Saitô).

0005-2736/$ - see front matter © 2006 Elsevier B.V. All rights reserved.
doi:10.1016/j.bbamem.2006.01.021

polarization-magic angle spinning (CP-MAS) NMR. These ^{13}C NMR signals are displaced upon their respective conformation, and in some instances, dynamics [13,14], but indifferent from intermolecular interactions, in contrast to ^{1}H and ^{15}N chemical shifts. Under such circumstance, site-directed assignment of peaks is feasible by locating the missing signal(s) in a site-directed mutant, in which certain residue of interest is replaced by another amino acid residue, with reference to ^{13}C NMR signals of wild type [13], provided that the introduced site-directed mutation does not induce any global conformational change. The assigned ^{13}C NMR peaks thus obtained can be utilized as intrinsic probe for local conformational and dynamics characterization [13].

These proteins from 2D or 3D crystals turned out to be not always rigid at *ambient temperature* as anticipated from current 3D structural models revealed by cryo-electron microscope or X-ray diffraction at *lower temperature*, but very flexible at fully hydrated state of biological relevance, in view of site-directed solid-state ^{13}C NMR, recorded by CP-MAS and single-pulse, dipolar decoupled-magic angle spinning (DD-MAS) technique: they undergo various kinds of molecular motions with fluctuation frequencies in the order of 10^2–10^8 Hz depending upon portions under consideration [13–16]. The resulting ^{13}C NMR signals are broadened or almost completely suppressed when their *incoherent* fluctuation frequencies (10^4–10^5 Hz) are interfered with coherent frequency of either proton decoupling (10^5 Hz) or magic angle spinning (10^4 Hz) or both, leading to failure of attempted peak-narrowing essential for achieving high-resolution solid-state NMR [17–19]. Here, the estimated frequencies in the order of 10^4 and 10^5 Hz should be borne in mind as corresponding to 4×10^3 and 5×10^4 Hz, respectively [20]. Therefore, several ^{13}C NMR signals from the loops or surface areas of the transmembrane α-helices turned out to be suppressed even in 2D crystalline bR preparations, if they were labeled with [1-^{13}C]Gly, Ala, Leu, Phe, Tyr, etc. with side-chains expressed by C_α–$C_\beta H_2$–X [12,15], because backbone dynamics could be coupled with a possible rotational motion of the χ_{II} angle around the C_α–C_β bond, although no such motion is involved in [1-^{13}C]Val- or Ile-labeled residues in which the side chain is expressed by C_α–C_β H(Y)(Z) [12]. Further, several ^{13}C NMR signals from the C- or N-terminal residues protruding from the membrane surface are preferentially suppressed by CP-MAS NMR, because their dipolar interactions are time-averaged due to the presence of (isotropic) fluctuation motions with frequency up to the order of 10^8 Hz.

Naturally, ^{13}C NMR spectral features of such membrane proteins could be modified, when the above-mentioned lipid–protein and protein–protein interactions are removed or modified as in disrupted (reconstituted in lipid bilayers present as monomers) [21], or distorted 2D crystals (modified lipid–protein or protein–protein interactions or modified electronic charges in the counter ion or surface residues for a variety of bR mutants) [22–25]. Biological activity for a number of membrane proteins is also retained in detergent micelles present as a monomer. Indeed, proton pump activity of reconstituted bR in lipid bilayer turned out to be native-like [26]. It turned out that fluctuation frequencies of the transmembrane α-helices and loops in reconstituted bR in lipid bilayers were increased from 10^2 and 10^4 Hz for 2D crystals from PM, respectively to 10^4 and 10^5 Hz [16,21–25]. As a result, ^{13}C NMR signals from the loops and several transmembrane α-helical regions of membrane proteins could be preferentially suppressed by interference of incoherent fluctuation frequencies with coherent frequencies of proton decoupling or magic angle spinning, when they are reconstituted into lipid bilayers [16,21] or present as distorted 2D crystals such as W80L and W12L mutants [22].

Utilization of membrane proteins overexpressed in *E. coli* and reconstitution in lipid bilayers are inevitable for their ^{13}C NMR studies, together with search for endogenous lipid component to promote such crystalline structure of a number of membrane proteins [16,20,27,28] because their 3D crystallization is generally extremely difficult. In particular, bR and its mutants can be used as ideal model systems suitable for this purpose, because a comparative study on both naturally occurring 2D crystal and reconstituted samples in lipid bilayers are readily available. In this connection, it is also very interesting to clarify whether or not modified ^{13}C NMR spectral feature of D85N is really a consequence of a distorted 2D crystalline lattice as proposed [23,24] with reference to the data of highly modified system such as reconstituted preparation in lipid bilayers.

In this paper, we aimed to gain a clue as to the following questions with expectation to reveal conformation and dynamics changes in D85N in lipid bilayers by ^{13}C NMR studies with reference to those of 2D crystalline preparations: (1) how can ^{13}C NMR spectra of [3-^{13}C]Ala or [1-^{13}C]Val-labeled D85N in reconstituted in lipid bilayers be distinguished from those of wild type bR from PM, as a result of concomitant major global conformational change triggered by neutralization of a single electronic charge at Asp 85? (2) How can conformational changes of D85N taking M-like intermediate at pH 10 be distinguished from those of ^{13}C NMR spectra recorded at pH 7 in lipid bilayer? (3) Under what condition, can ^{13}C NMR spectra of D85N 2D crystals be achieved from preparations of reconstituted lipid bilayers? (4) How can conformation and dynamics of bR or D85N be modified in the presence of specific lipid–protein or protein–protein interactions?

2. Materials and method

L-[3-^{13}C]Alanine and [1-^{13}C]valine were purchased from CIL, Andover, USA and used without further purification. *H. salinurum* S9 and its mutant D85N were grown in TS medium of Ohnishi et al. [29], in which unlabeled L-alanine and L-valine were replaced by [3-^{13}C]Ala and [1-^{13}C]Val, respectively. Purple or blue membranes containing bR or mutant were isolated by the method of Oesterhelt and Stoeckenius [30] and concentrated by centrifugation at 40,000×*g*, 4 °C, and 60 min from its suspension in 10 mM HEPES, 10 mM NaCl, 0.025% (w/v) NaN_3 at pH 7. The resulting pellet was resuspended in the same buffer and centrifugation was repeated five times until supernatant was made transparent. D85N or bR were solubilized by adding 5% (w/v) n-decyl-β-maltoside (DM) solution, containing 20 mM MES and 0.025% (w/v) NaN_3 at pH 5.0 to pellets thus obtained while stirring in the dark at 40 °C. The solubilized D85N or bR thus obtained were mixed with multibilayers of egg PC or DMPC (1:50 for the protein to lipids) and reconstituted samples in lipid bilayer were

prepared by removing DM with Bio-beads (SM-2 Adsorbent, 20–50 mesh). D85N content was evaluated by absorption spectra using $\varepsilon_{605}=4.5\times10^4$ cm^{-1} M^{-1} at light-adapted state. This value was estimated from a relation, A_{568}(bR)/$\varepsilon_{568}=A_{605}$(D85N)/$\varepsilon_{605}$, by assuming that the protein concentration is the same under the identical absorption maximum at 280 nm from the aromatic side chain. The reconstituted reparations were further centrifuged at 415000×*g*, 60 min, and 4 °C several times. Reconstituted D85N at pH 10 was prepared by suspending D85N/PC sample in 20 mM CHES, 10 mM NaCl, 0.025% (w/v) NaN_3 at pH 10 and centrifugation three times. Absorption spectra were always checked immediately after each experimental step. The pellets thus obtained were placed into a 5-mm od.d. zirconia pencil-type rotor. The caps were tightly glued to the rotor by rapid Araldite® (Vantico) to prevent leakage of water from the sample during magic angle spinning for solid-state NMR experiments.

100.63 MHz ^{13}C NMR spectra of fully hydrated pelleted preparations of [3-^{13}C]Ala-, [1-^{13}C]Val-labeled D85N or bR were recorded in the dark at 20 °C on a Chemagnetics CMX 400 NMR spectrometer both by cross polarization-magic angle spinning (CP-MAS) and single-pulse excitation with dipolar decoupled-magic angle spinning (DD-MAS) method, to distinguish ^{13}C NMR signals of proteins arising from flexible N- and C-terminal residues protruding from the membrane surface [13,14]. Indeed, no ^{13}C NMR signals from such region are available from CP-MAS NMR spectra of fully hydrated membrane proteins. The spectral width, contact time and acquisition time for CP-MAS experiment were 40 kHz, 1 and 50 ms, respectively. This prolonged contact time (50 ms) turned out to be essential to completely sample long tail of FID from fully hydrated bR for better achievement of spectral resolution [31]. The 90° pulses for carbon and proton nuclei were 5 μs each for CP-MAS experiment and 45° pulse for carbon was used for DD-MAS experiment. Repetition times for the former and latter were 4 and 6 s, respectively. Free induction decays were acquired with data points of 2000. Fourier transform was carried out as 16,000 points after 14,000 points were zero-filled to improve digital spectral resolution. ^{13}C chemical shifts were initially referred to the carboxyl carbon signal of crystalline glycine (176.03 ppm from TMS) and converted to the value relative to TMS.

3. Results

Fig. 1 illustrates the ^{13}C CP-MAS NMR spectra of reconstituted [3-^{13}C]Ala-labeled D85N in egg PC bilayers recorded at pH 7 (A) and pH 10 (B), respectively, as compared with those of bR at pH 7 in egg PC bilayers (C) and from PM (D). It should be noted that the ^{13}C NMR spectra of [3-^{13}C]Ala-D85N reconstituted in egg PC bilayers are substantially suppressed as compared with those of bR (Fig. 1D) and D85N from PM [23]. The ^{13}C NMR signals from the loop are completely absent and the peak-intensities of the transmembrane α_{II}-helices are also substantially decreased [23]. These ^{13}C NMR signals are also suppressed in the DD-MAS NMR spectra as illustrated in Fig. 2, although the ^{13}C NMR peaks from the loop regions were overlapped with the intense ^{13}C NMR peaks from the C-terminal residues. This is mainly caused by that the ^{13}C CP-MAS and DD-MAS NMR signals of several loop, α_I- and α_{II}-helical portions of the transmembrane α-helices of D85N mutant are preferentially suppressed by failure of the attempted peak-narrowing by proton decoupling due to the presence of incoherent fluctuation frequency in the order of 10^5 Hz interfered with coherent frequency of the proton decoupling [14–17,23] as demonstrated also in the reconstituted wild type bR in egg PC bilayer (C). Surprisingly, underlying global conformation and dynamics changes of D85N by taking the M-like state without photo-illumination at pH 10 [32], however, cannot be distinguished from those of the ground state at pH 7 (Fig. 1A and B), although such change was readily

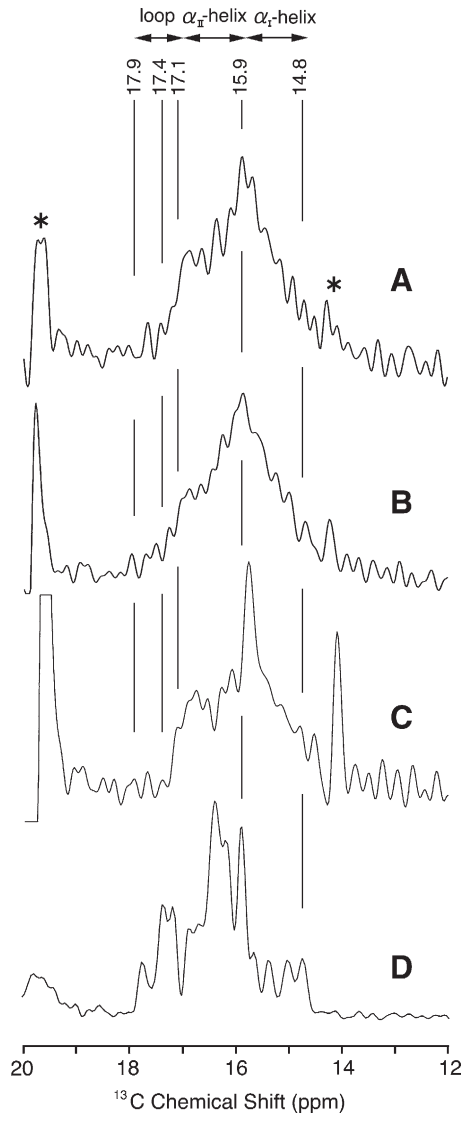

Fig. 1. ^{13}C CP-MAS NMR spectra of reconstituted [3-^{13}C]Ala-labeled D85N in egg PC bilayers at pH 10 (A), at pH 7 (B), and wild type reconstituted bacteriorhodopsin in egg PC bilayers at pH 7 (C) and wild type bacteriorhodopsin from PM. The asterisked peak at 19.8 ppm arises from the side methyl group of (3R, 7R, 11R)-15-tetramethylhexadecyl group of endogenous lipid from PM. The other asterisked peak at the high field region is ascribed to egg PC.

evaluated by ^{13}C NMR spectra as far as respective 2D crystalline preparations were compared [23,24].

It is noteworthy that the asterisked ^{13}C NMR peak at 19.8 ppm, arising from the transferred ^{13}C nuclei from [3-^{13}C] Ala to the side methyl groups of the (3R, 7R, 11R)-15-tetramethylhexadecyl group of lipids from PM [33], is characteristic of formation of either 2D crystal or monomeric forms. This peak is almost suppressed in the former but not in the latter. The intense 15.9 ppm peak, ascribable to the C-terminal α-helix of wild type bR in egg PC bilayers, is also suppressed to some extent in the CP-MAS NMR spectra of D85N mutant (Fig. 1A and B), but this peak is still the major peak as viewed from the reconstituted [3-^{13}C]Ala-D85N recorded by the ^{13}C DD-MAS NMR spectra (Fig. 2). This

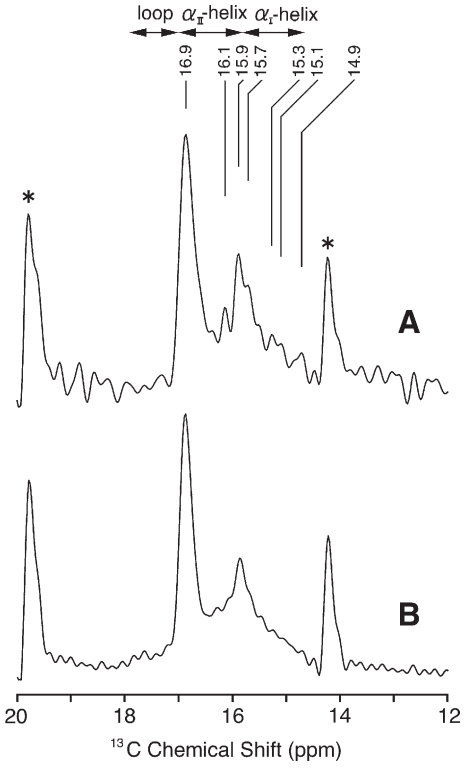

Fig. 2. ^{13}C DD-MAS NMR spectra of reconstituted [3-^{13}C]Ala-labeled D85N in egg PC bilayers at pH 10 (A) and at pH 7 (B).

portion is present as a state of fluctuation motion in the order of 10^6 Hz in wild type bR from PM [15].

We further recorded the ^{13}C NMR spectra of reconstituted [3-^{13}C]Ala-D85N mutant in DMPC bilayers at pH 7 at various temperatures (Fig. 3). The suppressed ^{13}C NMR peaks at the loops and transmembrane α_{II}-helices at ambient temperatures are substantially recovered at lower temperatures (0° to −5 °C), due to formation of 2D array under the presence of the endogenous lipid(s) from *Halobacteria* (asterisked peak) [34–36] tightly bound to D85N during isolation process. The recovery of the intense α_{II}-helical peak at 16.28 ppm is noteworthy at temperature below 0 °C (Fig. 3B), although the relative peak-intensities at this region are still not always the same as those of naturally occurring 2D crystals at this temperature. The intense peak at 15.94 ppm, arising from the C-terminal α-helix, is shifted upfield to 15.72 ppm when the temperature was lowered from 20° to −5 °C. Such an upfield displacement of the C-terminal α-helical peak was accompanied by reduced frequency of thermal fluctuations at low temperatures, because Ala C_β signals exhibit dynamics-dependent displacement of peaks [13]. Therefore, it is well recognized that this peak-position is not necessarily the same as that of 2D crystal at ambient temperature. It is also noteworthy that the ^{13}C NMR peak-intensity of the asterisked endogenous lipid(s) at 19.8 ppm is suppressed together with formation of 2D array as a result of modified dynamics at the lipid portion also, as a result of recovered lipid–protein interaction in the trimer structure.

The corresponding ^{13}C NMR spectra of [1-^{13}C]Val-labeled bR (A) and D85N (C) (upper traces) reconstituted in egg PC bilayers are compared with those of 2D crystalline preparations (B and D, respectively, bottom traces) as shown in Fig. 4. It is notable that most of the peaks, especially at the low field peaks from the transmembrane α-helices in lipid bilayer, are substantially suppressed, owing to the presence of fluctuation frequencies in the order of 10^4 Hz which could be interfered with frequency of magic angle spinning. Under such condition, it is very difficult to distinguish the ^{13}C NMR signals of [1-^{13}C]Val-D85N from those of bR (A and C) in spite of their obvious difference from 2D crystals (B and D). Backbone fluctuation frequencies for D85N and bR in lipid bilayer turned out to be in the order of 10^4–10^5 Hz because ^{13}C NMR peaks from [3-^{13}C]Ala- and [1-^{13}C]Val-labeled bR and D85N mutants are equally suppressed. As described already, however, the ^{13}C NMR signals from the loop regions of [3-^{13}C]Ala-labeled bR and D85N were more preferentially suppressed (Fig. 1). In contrast, it is interesting to note that the ^{13}C NMR signals of the transmembrane α-helices of [1-^{13}C]Val-labeled bR and D85N are more preferentially suppressed (Fig. 4A and C) as compared with those of the loop region because the fluctuation

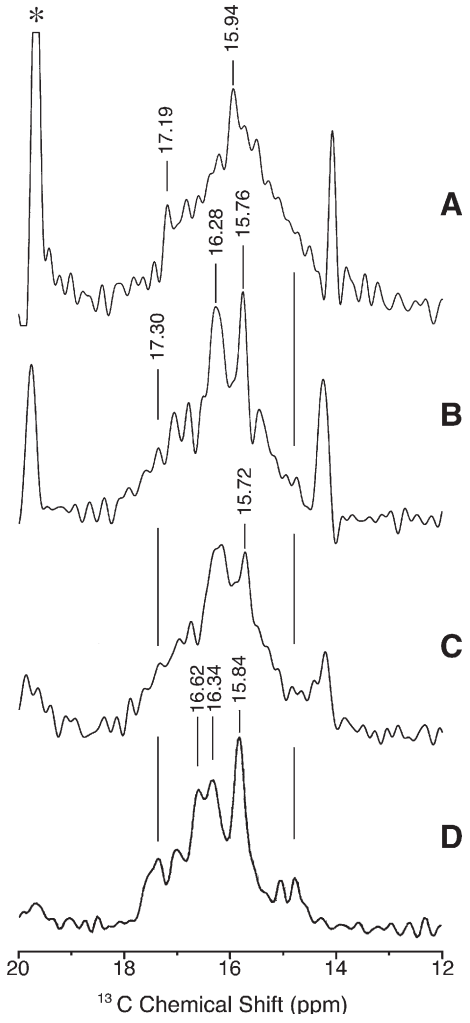

Fig. 3. ^{13}C CP-MAS NMR spectra of reconstituted [3-^{13}CAla]-labeled D85N in DMPC bilayers at pH 7 at various temperatures. 20 °C (A), 0 °C (B), −5 °C (C) and those of 2D crystalline preparations (D).

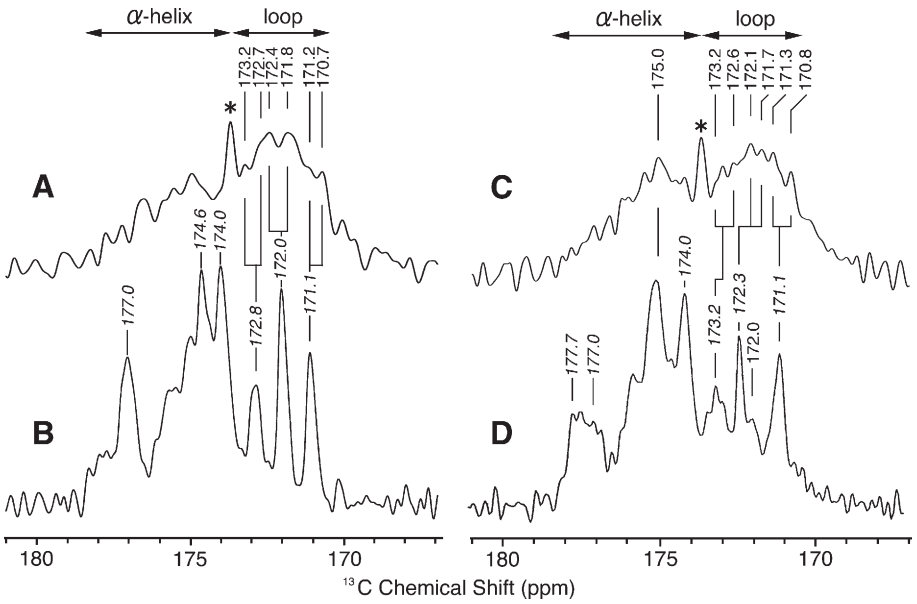

Fig. 4. ^{13}C NMR spectra for the carbonyl region of [1-^{13}C]Val-labeled bR (A) and D85N (C) reconstituted in egg PC bilayers are compared with those of 2D crystalline bR preparations (B) and D85N (D). The asterisked peak at the upper trace arises from egg PC bilayer.

frequency sensitive to the motions in this case is in the order of 10^4 Hz.

It appears that approximately six ^{13}C NMR peaks of [1-^{13}C]Val-labeled bR or D85N in the reconstituted preparations were resolved at the peak-positions for the loop region which are ascribed to the loop (Fig. 4A and C), although they are accidentally degenerated into the three (bR) and four (including a less intense peak at 172.0 ppm) peaks (D85N) in 2D crystalline state (Fig. 4B and D). This may be caused by a plausible conformational change induced by lipid–protein and protein–protein interactions, leading to formation of 2D crystal in the presence of the endogenous lipid(s) [24]. The assigned three intense ^{13}C NMR peaks at the loop region of [1-^{13}C]Val-bR for 2D crystalline bR, 171.0, 172.0 and 172.9 ppm, were ascribed to Val 101/199, 49/130, and 34/69, respectively [12]. The central single peak for bR from PM at 172.0 ppm peak (Val 49/130 for wild type bR) is split into two the asymmetric two peaks 173.2 and 172.0 ppm for D85N at pH 7, which were assigned to Val 49 and 130, respectively [24]. Naturally, the accidentally overlapped ^{13}C NMR peaks of either Val 101 or 199 of [1-^{13}C]Val-bR from PM may be resonated separately at different positions, if any constraint to do so is removed in reconstituted preparations. Further, the conformational change achieved in D85N mutant is reproducible to some extent in wild type bR, in which the single peak at 172.0 ppm is split into the two peaks in lipid bilayers. This is because such as lipid–protein and protein–protein interactions were removed in the reconstituted preparations.

We also recorded the ^{13}C NMR spectra of reconstituted [1-^{13}C]Val-labeled D85N in DMPC bilayers at various temperatures between 20° and −5 °C, as compared with the ^{13}C NMR spectrum of its 2D crystalline preparation (Fig. 5). Very low intense ^{13}C NMR spectrum was observed for [1-^{13}C]Val-D85N in DMPC bilayers at ambient temperature, as compared with that in egg PC bilayers: this is obviously caused by dynamics changes in the protein between egg PC and DMPC bilayers whose membrane fluidity substantially differs as viewed from their phase transition temperatures. Interestingly, most of the ^{13}C NMR feature as observed in 2D crystalline preparations was recovered at the temperature 0 °C, although complete recovery could be achieved at the temperature −15 °C as encountered for bR [12,21].

4. Discussion

4.1. Suppressed ^{13}C NMR signals due to conformation and dynamics changes by distorted or disrupted 2D crystalline lattice

The ^{13}C NMR spectra of reconstituted [3-^{13}C]Ala- and [1-^{13}C]Val-labeled D85N in egg PC bilayers at pH 7 are substantially suppressed with reference to those of wild type bR from PM, although the peak-intensity of the C-terminal α-helix is rather indifferent. Under such condition, the asterisked peak at 19.8 ppm, arising from the transferred ^{13}C nuclei from [3-^{13}C]Ala to the side methyl groups of (3R, 7R, 11R)-15-tetramethylhexadecyl group of the endogenous lipid from PM, is more pronounced because of acquired increased fluctuation frequency escaped from interference with the proton decoupling frequency. The present observation as well as our previous data [12–16,21–24] showed that the manner of such suppressed or recovered peaks strongly depends upon sample preparations (2D crystals, distorted or disrupted 2D lattice, or reconstituted samples, as summarized in Table 1), temperatures in relation to lipid phase [33], or a residue used as a probe (such as [1-^{13}C]Gly-, Ala-, Leu-, etc. labeled [12]). In particular, it is interesting to note that the spectral feature as recovered in reconstituted lipid bilayer is very similar to that of distorted or disrupted 2D lattice. As to fluctuation motions leading to the suppressed peaks, two kinds of protein dynamics should be distinguished:

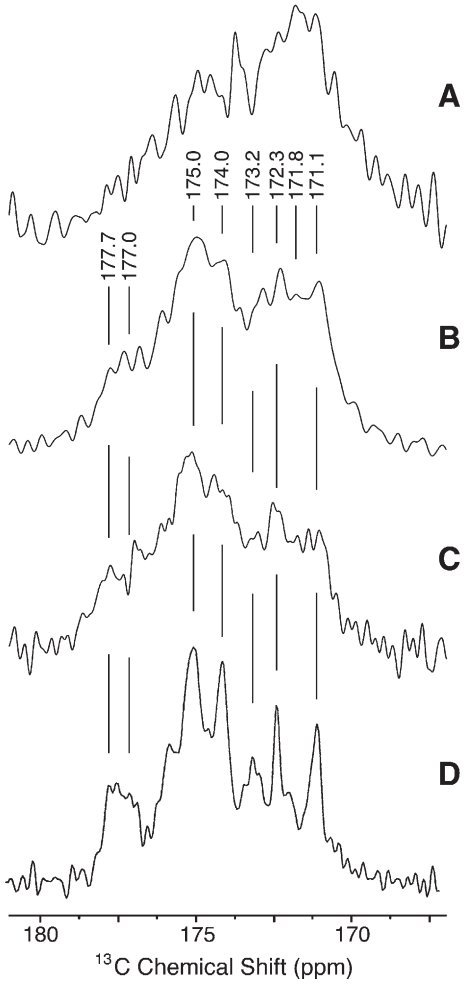

Fig. 5. ^{13}C CP-MAS NMR spectra of reconstituted [1-^{13}C]Val-labeled D85N in DMPC bilayers at pH 7 at various temperatures. 20 °C (A), 0 °C (B), −5 °C (C) and those of 2D crystalline preparations (D).

In the fast protein dynamics with fluctuation frequency in the order of 10^8 Hz, ^{13}C CP-MAS NMR signals, from the C-terminal end groups taking random coil conformation resonated at 16.9 ppm, are preferentially suppressed owing to isotropically averaged dipolar interactions, although the corresponding ^{13}C NMR signals were nevertheless fully visible from DD-MAS NMR. On the contrary, both ^{13}C CP-MAS and DD-MAS NMR signals are simultaneously suppressed as for peaks of some transmembrane α-helices (16–16.9 ppm) and loops (17.4–17.9 ppm) when fluctuation frequency is interfered with either frequency of the proton decoupling, magic angle spinning, or both [17–19]. Recording spectra by both CP-MAS and DD-MAS NMR at the same time is therefore essential to distinguish these two cases.

In the latter, the transverse relaxation time T_2^C values *under proton-decoupled MAS NMR* strongly depend on coherent frequencies of the proton decoupling or MAS which are interfered with incoherent frequency of molecular fluctuation motions. The overall relaxation rate, $1/T_2^C$ can be given by

$$1/T_2^C = (1/T_2^C)^S + (1/T_2^C)_{DD}^M + (1/T_2^C)_{CS}^M \quad (1)$$

where $(1/T_2^C)^S$ is the transverse component due to static C–H dipolar interactions, and $(1/T_2^C)_{DD}^M$ and $(1/T_2^C)_{CS}^M$ are the transverse components due to the fluctuation of the dipolar and chemical shift interactions respectively [17–19]. The latter two terms are given as a function of correlation time, τ_c, by

$$(1/T_2^C)_{DD}^M = \frac{4\gamma_I^2\gamma_S^2\hbar^2}{15r^6} I(I+1)\frac{\tau_c}{1+\omega_I^2\tau_c^2} \quad (2)$$

$$(1/T_2^C)_{CS}^M = \frac{\omega_0(\Delta\delta)^2\eta^2}{45}\left(\frac{\tau_c}{1+4\omega_r^2\tau_c^2} + \frac{2\tau_c}{1+\omega_r^2\tau_c^2}\right) \quad (3)$$

where γ_I and γ_S are the gyromagnetic ratios of the I and S nuclei, respectively, r is the internuclear distance between spins I and S, ω_0 and ω_r are the carbon resonance frequency and the amplitude of the proton decoupling Rf field respectively, ω_r is the rate of spinner rotation, $\Delta\delta$ is the CSA, and η is the asymmetric parameter of the chemical shift tensor. Therefore, the second and third terms, $(1/T_2^C)_{DD}^M$ and $(1/T_2^C)_{CS}^M$, dominate the $1/T_2^C$ if fluctuation motions are present, depending upon the frequency range of either 50 kHz (ω_I) or 4 kHz (ω_r),

Table 1
^{13}C NMR spectral features[a] of [3-^{13}C]Ala- or [1-^{13}C]Val-labeled bR and its mutants under various conditions

	2D crystalline preparations			Distorted or disrupted 2D crystals			Reconstituted in lipid bilayer	
	bR	D85N	bO[b]	bO[c]	W80L	W12L	bR	D85N
[3-^{13}C]Ala-labeled	+++	++[d]	++[d]	+	+	+	+	+
[1-^{13}C]Val-labeled	+++	++[e]	++	+	−	−	+	+
Trimeric structure evaluated by CD spectrum	Yes	Yes			Yes	No		
References	[11,12]	[23,24]	[37]	[37]	[22]	[22]	[21]	This work

[a] ^{13}C NMR signals are: +++, fully visible; ++, partially suppressed, +, over-all peaks were suppressed, especially at the loop and several transmembrane α_{II}-helices; −, completely suppressed.
[b] Bacterioopsin in which retinal was removed from bacteriorhodopsin.
[c] Bacterioopsin from retinal-deficient E1001 mutant.
[d] Signals from the loops and several transmembrane α_{II}-helices were partially suppressed.
[e] Only Val 130 at 172.0 ppm.

respectively. More quantitative treatment to deduce the correlation times τ_c based on Eqs. (1)–(3), however, is not easy because evaluation of the peak-intensities without such an interference is not always possible.

We previously showed that the most distinct changes in ^{13}C NMR spectra of reconstituted [3-^{13}C]Ala-D85N at neutral pH from 2D crystalline preparation are preferentially suppressed at 17.78 ppm (Ala 196 from the F–G loop; this peak was originally interpreted in terms of the displaced peak to the upper field [23]) and at 16.41 and 16.19 ppm (the transmembrane α_{II}-helices including Ala 215 of helix G and Ala 39 of helix B), respectively, with reference to those of 2D crystalline bR from PM [23]. The acquired fluctuation frequency in the order of 10^5 Hz due to neutralization of the negative electric charge at Asp 85 results in such suppressed peaks [23,24]. The resulting D85N spectrum in lipid bilayer in Fig. 1B is very similar to that of D85N from 2D crystal, although the extent of the suppressed peaks including overall spectral area is much pronounced in D85N in lipid bilayer than 2D crystals (see Table 1). We therefore concluded that the partially suppressed peaks in D85N from 2D crystalline preparation at neutral pH is caused by contribution of partially distorted 2D crystal as viewed from the suppressed overall spectral intensities (Table 1). The extent of distorted 2D lattice is only nominal, however, because the peak-intensity at 19.8 ppm is almost unchanged between bR and D85N mutant in 2D crystalline preparations.

More surprisingly, the observed spectral pattern is almost the same between the ground state at pH 7 and the M-like intermediate achieved at pH 10 (Fig. 1A and B), in spite of the presence of accompanied global conformational changes caused by the destabilized ground state structure upon loss of interaction of the positively charged Schiff base with anionic counter residue that forms the counter ion [32]. Further, the reduced peak-intensity was noted at 16.6 ppm for D85N from 2D crystalline preparation upon raising pH from 7 to 10 to deprotonate the Schiff base and also at 16.3 ppm (including Ala 53) and 15.6 ppm (including Ala 51) ascribable to dynamic changes in helices B and G [23]. It should be noted, however, that the corresponding reverse process of the above-mentioned spectral change at 16.6 ppm is clearly seen, concomitant with the formation of 2D array at low temperature (Fig. 3C). Accelerated local fluctuation motion of the transmembrane B and C α-helices which facilitates efficient proton uptake at Asp 96 at the M-like state was seen by ^{13}C NMR studies on [1-^{13}C] Pro-labeled D85N [24]. It is noteworthy that the expected spectral changes to be visualized in the reconstituted preparations due to formation of the M-like state, however, will be masked in the presence of similarly suppressed peak-intensities owing to fluctuation frequency arising from the completely disrupted 2D lattice (Fig. 1A and B, and also Table 1), if their resulting conformation and dynamics changes might be similar each other. The present observation indicates that the induced fluctuations for both bR and D85N reconstituted in lipid bilayers might be comparable to those induced for the M-like state of D85N in 2D crystal in which conformational and dynamics changes have been examined so far in more detail [23,24]. This is the reason why ^{13}C NMR spectra observed in the reconstituted preparations are unexpectedly insensitive to the expected conformational change by forming the M-like state of D85N. Accordingly, it is highly desirable to record ^{13}C NMR spectra at low temperature to gain insight into conformational changes between the ground and M-like states.

Similar but more pronounced changes were also present for the ^{13}C NMR spectra of [3-^{13}C]Ala-labeled bacterio-opsin (bO) prepared by either bleaching of bR by removing retinal or growing retinal-deficient E1001 strain (Table 1) because their 2D lattice structures may be partly distorted or completely disrupted for the former and latter, respectively [37]. In fact, ^{13}C NMR spectra of [3-^{13}C]Ala-bO from the latter showed much broadened linewidths than those of bO from the former, because 2D lattice structure cannot be formed in the absence of retinal. Without helix–helix contact in monomers, it is expected that seven transmembrane α-helices and subsequent interhelical loops undergo fluctuation motions with frequency in the order of 10^4 Hz as estimated from the manner of the peak-suppression. In the absence of such specific Schiff base-counter ion interaction (M-like state or bO), transmembrane helices acquire fluctuation motions with frequency of 10^4 Hz, especially at B, F, G, and C helices, etc. Naturally, this kind of motions cannot be selectively detected in monomeric state in lipid bilayers.

At present, it is not possible to define the manner of the aforementioned motions in more detail based upon the present findings. One possibility for a mode of motion is a libration motion [38,39] of the two-site jump about the C_α–C'_α axis present even in the well-packed crystalline peptide, the correlation time of which was estimated to be 2.3×10^{-4} s at ambient temperature for crystalline Gly–Gly [38]. It is expected that this kind of motion could be also present even in the transmembrane α-helices either in 2D crystalline or monomers in lipid bilayers.

4.2. A possible conformation and dynamics change of D85N and bR due to the presence of 2D array

Low temperature NMR studies at around −10 °C gave rise to the ^{13}C NMR spectra of reconstituted [3-^{13}C]Ala-/[1-^{13}C] Val-labeled D85N preparations in gel-phase DMPC bilayers which are comparable to those of 2D crystalline preparations (Figs. 3 and 5). This is consistent with the previous findings for wild type bR in DMPC bilayer at −15 °C [12,21] but more pronounced in DPPC bilayer for ^{13}C NMR spectra of [3-^{13}C]Ala-/[1-^{13}C]Val-labeled bR at 0 °C in DPPC bilayers [21]. This is because the reduced temperature as defined by $T_R=(T-T_c)/T_c$ at $T=0$ °C for DPPC bilayers is lower than that at −10 °C for DMPC bilayers. Here, T_c is the phase transition temperature for pure lipid bilayer which is 23° and 43 °C for DMPC and DPPC bilayers, respectively, and T is the temperature at which spectra were recorded. Naturally, this is the consequence for formation of 2D lattice assembly at low temperature in the presence of endogenous lipid(s) from *Halobacteria* as manifested from the asterisked peak at 19.8 ppm [34–36]. The present experimental finding, together with that of our previous data [21], shows that the suppressed

peak-intensity of the side methyl group of the endogenous lipid at 19.8 ppm could be considered as an excellent probe for lowered fluctuation-frequency change to the order of 10^5 Hz in the environment of the side methyl group in the lipid in the 2D lattice. In contrast to naturally occurring 2D lattice from PM, this 2D array or lattice achieved at low temperature is not any more retained when temperature was again raised to ambient temperature, however.

The deceptively simplified spectral patterns in the three ^{13}C NMR signals of the loop regions in [1-^{13}C]Val-labeled D85N and bR from 2D crystalline preparations of PM arose from the accidental overlaps of the individual peaks consisting of two kinds of signals, although the central peak of bR from PM at 172.0 ppm (Val 49 and 130) are split into the asymmetric doublet (172.3 and 172.0 ppm, respectively) in the reconstituted D85N preparation in egg PC bilayers, the former peak of which being suppressed at the M-like state of the 2D preparation as a result of fluctuation motion of the helix B at which Val 49 is located [24]. It is noteworthy that the single peak resonated at 171.1 ppm in bR from PM [Val 101 (C–D loop) and 199 (F–G loop)] is split into the two peaks at 170.7 or 170.8 ppm (Fig. 4A and C) in the absence of the lipid–protein and protein–protein interactions in the reconstituted preparation as in egg PC bilayers at ambient temperature. It is interesting to note that this occurs also in wild type bR (Fig. 4A) when steric constraint from such helix–helix contact is removed in the reconstituted preparations [21]. Together with the major dynamics changes as observed from ^{13}C NMR spectra of [3-^{13}C]Ala-labeled bR [13,21,22], this is the first observation to exhibit the direct evidence for significant alteration in the conformations perturbed in the presence or absence of the helix–helix contact in oligomerized membrane proteins.

Nevertheless, it is also noteworthy that the ^{13}C NMR signal from the cytoplasmic α-helix protruding from the membrane surface is not strongly influenced by the manner of sample preparation either 2D crystal or monomer. This observation is very important because reconstitution of membrane proteins in lipid bilayers can be an excellent means to probe correctly the biologically important event occurring at the membrane surface such as the cytoplasmic surface complex consisting of the C-terminal α-helix and nearby loops [40] and signal transduction in the phototaxis sensory rhodopsin [41,42].

5. Concluding remarks

We found that the global conformation and dynamics changes occurring at the M-like state of 2D crystalline D85N at pH 10 are also visible for bR and D85N reconstituted in lipid bilayers at neutral pH. This is because ^{13}C NMR peaks of the peaks at the loop and some transmembrane α-helices, which are sensitive to such conformational and dynamics changes, are suppressed already by fluctuation motions in the order of 10^4 to 10^5 Hz interfered with frequencies of magic angle spinning or proton decoupling. Therefore, they behave as if they are not sensitive to the conformational and dynamics changes for D85N in lipid bilayers. Under such circumstances, one should always take into account of a possibility of missing signal caused by slow fluctuation motions, as far as ^{13}C NMR spectra of membrane proteins reconstituted in lipid bilayers were examined at ambient temperature. Nevertheless, it is emphasized that ^{13}C NMR signal of the C-terminal α-helix protruding from the surface is less sensitive to the manner of sample preparations and can be utilized as an excellent intrinsic probe for this portion. One way to recover the suppressed peak-intensities of the transmembrane α-helics and loops from the samples in lipid bilayer is to record ^{13}C NMR spectra at lower temperature at which 2D array of proteins under consideration is achieved, if a suitable endogenous lipid component to promote formation of 2D array is present as in bR from PM. The other way is to choose optimal spectrometer condition to avoid such interference of fluctuation frequency with proton decoupling or magic angle spinning, either by recording spectra at higher magnetic field or spinning rate.

References

[1] B.J. Bormann, D.M. Engelman, Intramembrane helix–helix association in oligomerization and transmembrane signaling, Annu. Rev. Biophys. Biomol. Struct. 21 (1992) 223–242.
[2] M.H. Stowell, D.C. Rees, Structure and stability of membrane proteins, Adv. Protein Chem. 46 (1995) 279–311.
[3] N. Grigorieff, T.A. Ceska, K.H. Dowing, J.M. Baldwin, R. Henderson, J. Mol. Biol. 259 (1996) 393–421.
[4] E. Pebay-Peyroula, G. Rummel, J.P. Rosenbusch, E.M. Landau, X-ray structure of bacteriorhodopsin at 2.5 Å from microcrystals grown in lipidic cubic phases, Science 277 (1997) 1676–1681.
[5] H. Luecke, H.R. Richter, J.K. Lanyi, Proton transfer pathways in bacteriorhodopsin at 2.3 Å resolution, Science 280 (1998) 1934–1937.
[6] E.R.S. Kunji, E.N. Spudich, R. Grisshammer, R. Henderson, J.L. Spudich, Electron crystallographic analysis of two-dimensional crystals of sensory rhodopsin II: a 6.9 A projection structure, J. Mol. Biol. 308 (2001) 279–293.
[7] H. Luecke, B. Schobert, J.K. Lanyi, E.N. Spudich, J.L. Spudich, Crystal structure of sensory rhodopsin II at 2.4 Å: insights into color tuning and transducer interaction, Science 293 (2001) 1499–1503.
[8] A. Royant, P. Nollert, K.L. Edman, R. Neutze, E.M. Landau, E. Pebay-Peyroula, J. Navarro, X-ray structure of sensory rhodopsin II at 2.1-Å resolution, Proc. Natl. Acad. Sci. U. S. A. 98 (2001) 10131–10136.
[9] J. Deisenhofer, O. Epp, K. Miki, R. Huber, H. Michel, Structure of the protein subunits in the photosynthetic reaction centre of *Rhodopseudomonas viridis* at 3 Å resolution, Nature 318 (1985) 618–624.
[10] M.P. Krebs, T.A. Isenberger, Structural determinants of purple membrane assembly, Biochim. Biophys. Acta 1460 (2000) 15–26.
[11] S. Tuzi, S. Yamaguchi, A. Naito, R. Needleman, J.K. Lanyi, H. Saitô, Conformation and dynamics of [3-^{13}C]Ala-labeled bacteriorhodopsin and bacterioopsin, induced by interaction with retinal and its analogs, as studied by ^{13}C nuclear magnetic resonance, Biochemistry 35 (1996) 7520–7527.
[12] H. Saitô, J. Mikami, S. Yamaguchi, M. Tanio, A. Kira, T. Arakawa, K. Yamamoto, S. Tuzi, Site-directed ^{13}C solid-state NMR studies on membrane proteins: strategy and goals toward revealing conformation and dynamics as illustrated for bacteriorhodopsin labeled with [1-^{13}C] amino acid residues, Magn. Reson. Chem. 42 (2004) 218–230.
[13] H. Saitô, S. Tuzi, M. Tanio, A. Naito, Dynamic aspect of membrane proteins and membrane-associated peptides as revealed by ^{13}C NMR: lessons from bacteriorhodopsin as an intact protein, Annu. Rep. NMR Spectrosc. 47 (2002) 39–108.
[14] H. Saitô, S. Tuzi, S. Yamaguchi, M. Tanio, A. Naito, Conformation and backbone dynamics of bacteriorhodopsin revealed by ^{13}C NMR, Biochim. Biophys. Acta 1460 (2000) 39–48.

[15] S. Yamaguchi, S. Tuzi, K. Yonebayashi, A. Naito, R. Needleman, J.K. Lanyi, H. Saitô, Surface dynamics of bacteriorhodopsin as revealed by ^{13}C NMR studies on [^{13}C]Ala-labeled proteins: detection of millisecond or microsecond motions in interhelical loops and C-terminal α-helix, J. Biochem. (Tokyo) 129 (2001) 373–382.
[16] H. Saitô, Dynamic pictures of membrane proteins in two-dimensional crystal, lipid bilayer and detergent as revealed by site-directed ^{13}C NMR, Chem. Phys. Lipids 132 (2004) 101–112.
[17] W.P. Rothwell, J.S. Waugh, Transverse relaxation of dipolar coupled spin systems under rf irradiation: detection motions in solid, J. Chem. Phys. 75 (1981) 2721–2732.
[18] D. Suwelack, W.P. Rothwell, J.S. Waugh, Slow molecular motion detected in the NMR spectra of rotating solids, J. Chem. Phys. 73 (1980) 2559–2569.
[19] A. Naito, A. Fukutani, M. Uitdehaag, S. Tuzi, H. Saitô, Backbone dynamics of polycrystalline peptides studied by measurements of ^{15}N NMR lineshapes and ^{13}C transverse relaxation times, J. Mol. Struct. 441 (1998) 231–241.
[20] S. Yamaguchi, K. Shimono, Y. Sudo, S. Tuzi, A. Naito, N. Kamo, Conformation and dynamics of the [3-^{13}C]Ala, [1-^{13}C]Val-labeled truncated *pharaonis* transducer, *p*HtrII (1–159), as revealed by site-directed ^{13}C solid-state NMR: changes due to association with phoborhodopsin (sensory rhodopsin II), Biophys. J. 86 (2004) 3131–3140.
[21] H. Saitô, K. Yamamoto, S. Tuzi, S. Yamaguchi, Backbone dynamics of membrane proteins in lipid bilayers: the effect of two-dimensional array formations as revealed by site-directed solid-state ^{13}C NMR studies on [3-^{13}C]Ala and [1-^{13}C]Val- labeled bacteriorhodopsin, Biochim. Biophys. Acta 1616 (2003) 127–136.
[22] H. Saitô, T. Tsuchida, K. Ogawa, T. Arakawa, S. Yamaguchi, S. Tuzi, Residue-specific millisecond to microsecond fluctuations in bacteriorhodopsin induced by disrupted or disorganized two-dimensional crystalline lattice, through modified lipid–helix and helix–helix interaction, as revealed by ^{13}C NMR, Biochim. Biophys. Acta 1565 (2002) 97–106.
[23] Y. Kawase, M. Tanio, A. Kira, S. Yamaguchi, S. Tuzi, A. Naito, M. Kataoka, J.K. Lanyi, R. Needleman, H. Saitô, Alteration of conformation and dynamics of bacteriorhodopsin induced by protonation of Asp 85 and deprotonation of Schiff base as studied by ^{13}C NMR, Biochemistry 39 (2000) 14472–14480.
[24] A. Kira, M. Tanio, S. Tuzi, H. Saitô, Significance of low-frequency local fluctuation motions in the transmembrane B and C α-helices of bacteriorhodopsin, to facilitate efficient proton uptake from the cytoplasmic surface, as revealed by site-directed sold-state ^{13}C NMR, Eur. Biophys. J. 33 (2004) 580–588.
[25] H. Saitô, S. Yamaguchi, K. Ogawa, S. Tuzi, M. Márquez, C. Sanz, E. Padrós, Glutamic acid residues of bacteriorhodopsin at the extracellular surface as determinants for conformation and dynamics as revealed by site-directed solid-state ^{13}C NMR, Biophys. J. 86 (2004) 1673–1681.
[26] K.S. Huang, H. Bayleyn, M.J. Liao, E. London, H.G. Khorana, Refolding of an integral membrane protein. Denaturation, renaturation, and reconstitution of intact bacteriorhodopsin and two proteolytic fragments, J. Biol. Chem. 256 (1981) 3802–3809.
[27] T. Arakawa, K. Shimono, S. Yamaguchi, S. Tuzi, Y. Sudo, N. Kamo, H. Saitô, Dynamic structure of *pharaonis* phoborhodopsin (sensory rhodopsin II) and complex with a cognate truncated transducer as revealed by site-directed ^{13}C solid-state NMR, FEBS Lett. 536 (2003) 237–240.
[28] S. Yamaguchi, S. Tuzi, J.U. Bowie, H. Saitô, Secondary structure and backbone dynamics of *Escherichia coli* diacylglycerol kinase, as revealed by site-directed solid-state ^{13}C NMR, Biochim. Biophys. Acta 1698 (2004) 97–105.
[29] H. Onishi, M.E. McCance, N.E. Gibbons, A synthetic medium for extremely halophilic bacteria, Can. J. Microbiol. 11 (1965) 365–373.
[30] D. Oesterhelt, W. Stoeckenius, Isolation of the cell membrane of *Halobacterium halobium* and its fractionation into red and purple membrane, Methods Enzymol. 31 (1974) 667–678.
[31] S. Tuzi, S. Yamaguchi, M. Tanio, H. Konishi, S. Inoue, A. Naito, R. Needleman, J.K. Lanyi, H. Saitô, Location of a cation-binding site in the loop between helices F and G of bacteriorhodopsin as studied by ^{13}C NMR, Biophys. J. 76 (1999) 1523–1531.
[32] L.S. Brown, H. Kamikubo, L. Zimanyi, M. Kataoka, F. Tokunaga, P. Verdegem, J. Lugtenburg, J.K. Lanyi, A local electrostatic change is the cause of the large-scale protein conformation shift in bacteriorhodopsin, Proc. Natl. Acad. Sci. U. S. A. 94 (1997) 5040–5044.
[33] S. Tuzi, A. Naito, H. Saitô, Temperature-dependent conformational change of bacteriorhodopsin as studied by solid-state ^{13}C NMR, Eur. J. Biochem. 239 (1996) 294–301.
[34] B. Sternberg, P. Gale, A. Watts, The effect of temperature and protein content on the dispersive properties of bacteriorhodopsin from *H. halobium* in reconstituted DMPC complexes free of endogenous purple membrane lipids: a freeze-fracture electron microscopy study, Biochim. Biophys. Acta 980 (1989) 117–126.
[35] B. Sternberg, C. L'Hostis, C.A. Whiteway, A. Watts, The essential role of specific *Halobacterium halobium* polar lipids in 2D-array formation of bacteriorhodopsin, Biochim. Biophys. Acta 1108 (1992) 21–30.
[36] A. Watts, Bacteriorhodopsin: the mechanism of 2D-array formation and the structure of retinal in the protein, Biophys. Chem. 55 (1995) 137–151.
[37] S. Yamaguchi, S. Tuzi, M. Tanio, A. Naito, J.K. Lanyi, R. Needleman, H. Saitô, Irreversible conformational change of bacterio-opsin induced by binding of retinal during its reconstitution to bacteriorhodopsin, as studied by ^{13}C NMR, J. Biochem. (Tokyo) 127 (2000) 861–869.
[38] A. Naito, A. Fukutani, M. Uitdehaag, S. Tuzi, H. Saitô, Backbone dynamics of polycrystalline peptides studied by measurements of ^{15}N NMR lineshapes and ^{13}C transverse relaxation times, J. Mol. Struct. 441 (1998) 231–241.
[39] K.J. Hallock, D.K. Lee, A. Ramamoorthy, The effects of librations on the ^{13}C chemical shift and ^{2}H electric field gradient tensors in β-calcium formate, J. Chem. Phys. 113 (2000) 11187–11193.
[40] K. Yonebayashi, S. Yamaguchi, S. Tuzi, H. Saitô, Cytoplasmic surface structures of bacteriorhodopsin modified by site-directed mutations and cation binding as revealed by ^{13}C NMR, Eur. Biophys. J. 32 (2003) 1–11.
[41] T. Arakawa, K. Shimono, S. Yamaguchi, S. Tuzi, Y. Sudo, N. Kamo, H. Saitô, Dynamic structure of *pharaonis* phoborhodopsin (sensory rhodopsin II) and complex with cognate truncated transducer as revealed by site-directed ^{13}C solid-state NMR, FEBS Lett. 536 (2003) 237–240.
[42] S. Yamaguchi, K. Shimono, Y. Sudo, S. Tuzi, A. Naito, N. Kamo, H. Saitô, Conformation and dynamics of the [3-^{13}C]Ala, [1-^{13}C]Val-labeled truncated *pharaonis* transducer, *p*HtrII (1–159), as revealed by site-directed ^{13}C solid-state NMR: changes due to association with phoborohodopsin (sensory rhodopsin II), Biophys. J. 86 (2004) 3131–3140.